

Modeling and Testing of a Novel Piezoelectric Pump

John Jansen, Randal Lind, Lonnie Love, and Joel Chesser
Oak Ridge National Laboratory
P.O. Box 2008, MS-6305
Oak Ridge, TN 37831

Abstract- While there is a wide range of actuation technologies, none currently rivals the overall performance (power density, bandwidth, stress, stroke) of conventional hydraulic actuation [1]. It is well known in the actuation community that the power-to-weight ratios and the power-to-volume ratios of hydraulic actuators are, respectively, around 5 times and 10 to 20 times larger than comparable electric motors. Due to fundamental limitations in the magnetic flux density in the supporting structures and limitations in the heat transfer out of electric actuators, significant changes in these ratios are not likely in the near future [2]. Thermal limitations associated with electric motors do not apply to hydraulic actuators since the hydraulic fluid cools and lubricates the system. However, with all of these virtues, hydraulic actuators have serious practical implementation problems. Typically, servo-based hydraulic actuators are leaky and have generally poor energy efficiencies. This work addresses a new type of electric actuator that combines the best of both the electric and hydraulic mediums.

1. MOTIVATION

The goal of this paper is to discuss a novel actuator developed at Oak Ridge National Laboratory (ORNL) that has the potential to make piezoelectric materials a driving source for a new type of hydraulic actuator. Currently, the power-to-weight ratios of hydraulic actuators are around 5 times and the power-to-volume ratios are 10 to 20 times that of comparable electric motors [1]. The long-term goal of this project is a new actuator that exceeds the current level of power and volume density of electric motors and results in performance comparable to conventional hydraulics. While this goal has yet to be achieved, the research has resulted in the construction of a working pump capable of producing 32 W of mechanical power out with dead head pressures greater than 1000 psi.

One difficulty of using piezoelectric material pertains to converting small displacements to large motion (i.e., transmission problem). The approach taken in this research is to move small drops of fluid [3] at very high frequencies where the accumulation of small drops of fluid at a high rate adds up to a large flow rate. Precision control would be possible since small drops of fluids are incrementally controlled during each pump cycle. In addition, the energy efficiency compared to conventional hydraulic servo control applications could be vastly improved since no pressure drop across a servo valve would be required. This approach has

the potential of achieving the radical improvement in motion control for a high-power density actuator. A more detailed description of this pump can be found in [4].

2. BACKGROUND DISCUSSION

Large forces and small displacements occur in a piezoelectric crystal when an electric field is applied. Compressive stress levels can be as high as 35 MPa (5000 psi), whereas the tensile stress levels can be only 5 to 10% of the compressive stress level. An overview drawing of the basic pump concept is shown in Fig. 1. Note that the pump could be placed inside the actuator making the overall system self-contained and thereby significantly minimizing fluid leakage.

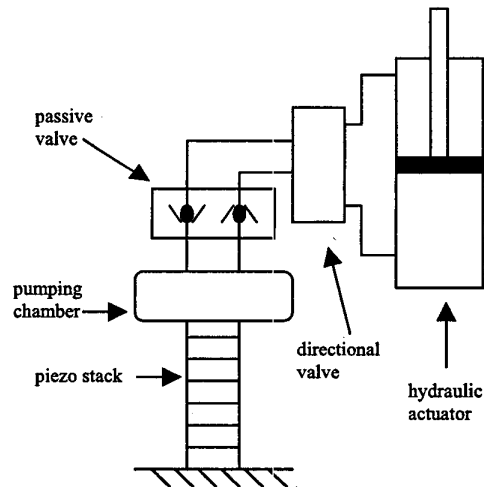


Figure 1: Simplified Pump and Actuator (the pump could possibly be placed inside the actuator)

A detail discussion of mechanical design issues such as stroke dimensions, fluid compressibility, and valving have been addressed elsewhere [4]. Due to space limitations, only a brief summary of the salient design issues will be provided here. First, fluid particle contaminants will be kept below 25 μm in size with standard filtration techniques. Since the stroke displacement is $> 100 \mu\text{m}$, fluid particle contaminants and machining will not be a problem. Next, the question is

how much of the stroke of the pump is required to compress the fluid assuming a system pressure of 2000 psi (2000 psi value was picked as an example) is applied. Assuming a stroke length of 75 μm and a typical fluid bulk modulus of 100,000 psi, only 1.5 μm out of 75 μm of the stroke is required to compress the fluid (see [4] for details). Under proper control, fluid compression has not been a significant problem if aeration issues in the fluid are carefully controlled. Lastly, the valves shown in Fig. 1 must operate around 1 kHz for allow the pump to rival the power density of a hydraulic actuator. Only passive valving was examined due to the tremendous compactness advantages it offers in the overall design. To achieve passive valving that can respond to 1 kHz, small distributive mini-valves (see Figs. 4 and 5) were designed instead of one large valve for each of the inlet and outlet flow directions so that the effective mass of each valve is small. Mini-valves for each inlet and outlet flow directions are distributed around the circumference of the pumping chamber. The natural frequency of each inlet and outlet valve has been tested and is over 2.2 kHz, which exceeds the 1 kHz operating frequency by over a factor of 2. Finally, piezoelectric actuators are driven by a high-voltage power source of around 400 to 1000 V. The size of the drive electronics often exceeds the overall packaging volume of the actuator by an order-of-magnitude. Currently, we are addressing this issue and the results will be forth coming in a later paper.

3. MODELING

3.1 Overview

There are five areas that need to be modeled to be able to understand and to predict the response of the proposed piezoelectric pump. These areas are the piezoelectric stack, the pumping chamber, the structure supporting the stack and chamber, the hydraulic load (a hydraulic cylinder in our case), and the distributive passive valves. Again due to space only the salient features of each of the modeling components will be addressed.

3.2 Piezoelectric Stack Model

A linear model for the piezoelectric stack that has current (or charge) and mechanical force as the input variables and the mechanical velocity and displacement as the output variables was chosen. The constitutive relations [5,6] for piezoelectric material are typically expressed in a tensor formulation as:

$$S_p = s_{pq}^E T_q + d_{kp} E_k \quad (1)$$

and

$$D_i = d_{iq} T_q + \epsilon_{ik}^T E_k \quad (2)$$

where S represents the strain tensor, s^E is the elastic compliance matrix constrained to a constant electric field, T

represents the stress tensor, d is the matrix of piezoelectric material coefficients, and ϵ^T is the permittivity matrix constrained to a constant stress. For the material used in this study, all the stresses and fields are limited to the 3-direction and the constitutive relationship can be approximated by

$$S_3 = s_{33}^E T_3 + d_{33} E_3 \quad (3)$$

and

$$D_3 = d_{33} T_3 + \epsilon_{33}^T E_3 \quad (4)$$

where the s_{33}^E , d_{33} , ϵ_{33}^T are now all scalars. Let $S_3 = x/t$, $D_3 = Q/A$, $E_3 = V/t$, $T_3 = F/A$ where x is the displacement of a single stack, t is the thickness of a single stack, Q is the charge on a single stack, V is the voltage on a stack, F is the applied load, A is the stack cross-sectional area. Define the total displacement of N stack in series as $x_T = Nx$ and define a load force, F , as $F = -Z_m \dot{x}_T - F_s$ where Z_m is a passive load impedance (this passive load will be replaced with a more detailed nonlinear model in later sections but is shown just for convenience) and F_s is an external force. After some algebraic exercise the results are similar to other researchers,

$$I_t = sQ_t = \frac{NA}{t} \left(\frac{\epsilon_{33}^T}{s_{33}^E} - \frac{d_{33}^2}{s_{33}^E} \right) sV + \frac{\left(\frac{NA}{t} \frac{d_{33}^2}{s_{33}^E} \right) sV}{1 + \left(\frac{NA}{t} \frac{d_{33}^2}{s_{33}^E} \right) \left(\frac{ts_{33}^E}{Ad_{33}} \right)^2 Z_m s} + \frac{\left(\frac{NA}{t} \frac{d_{33}^2}{s_{33}^E} \right) \left(\frac{ts_{33}^E}{Ad_{33}} \right) F_s}{1 + \left(\frac{NA}{t} \frac{d_{33}^2}{s_{33}^E} \right) \left(\frac{ts_{33}^E}{Ad_{33}} \right)^2 Z_m s} \quad (5)$$

or in a more condensed form as

$$I_t = sC_1 V + \frac{sC_2 (V - T F_s)}{1 + sC_2 T^2 Z_m} \quad (6)$$

where

$$C_0 = \frac{NA}{t} \epsilon_{33}^T, \quad (7)$$

$$C_1 = C_0 (1 - k^2), \quad (8)$$

$$C_2 = C_0 k^2, \quad (9)$$

$$k^2 = \frac{d_{33}^2}{\epsilon_{33}^T s_{33}^E}, \quad (10)$$

and

$$T' = \frac{ts_{33}^E}{Ad_{33}} \quad (11)$$

Equation 6 has an equivalent linear circuit representation as shown in Fig. 2 where C_1 and C_2 terms represent capacitive elements, T' is the turns ratio of a transformer that links the electrical model on the left port to the mechanical model on the right port of the transformer.

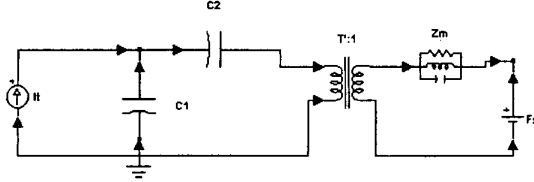


Figure 2. Linear piezoelectric stack model with load.

To accommodate for stack losses and how the electric permittivity of the piezoelectric material varies with voltage can be readily added to the above model by adding a shunt resistive element across C_1 to account for stack losses and by making the shunt and series capacitors voltage dependent [4].

3.3 Pumping Chamber Model

Standard fluid compliance relationships [7] have been found to be successful to model the pumping chamber. Proper de-aeration of the hydraulic fluid is critical for these models to be accurate. The pumping area is A and it's assumed that the outlet and inlet ports are closed (i.e., the chamber is deadheaded). By the definition of the fluid bulk modulus,

$$\beta = \frac{-V_0}{\Delta V} \Delta P \quad (12)$$

which can be manipulated through the following steps to arrive at the equivalent chamber stiffness, K_f :

$$\Delta V = -A \Delta x = \frac{-V_0}{\beta} \Delta P \quad (13)$$

$$-A \Delta x = \frac{-L}{\beta} \Delta F \quad (14)$$

$$\frac{\beta A}{L} \Delta x = \Delta F \quad (15)$$

and

$$K_f \Delta x = \Delta F \quad (16)$$

When the fluid chamber is deadheaded, the fluid looks like a simple spring of stiffness $K_f = \beta A/L$. The equivalent

capacitance of the chamber transferred to the left of the transformer and can be shown to be equivalent to

$$C'_m = \frac{1}{T'^2 K_f} \quad (17)$$

Likewise mass would look like an inductor to the left of the transfer and can be calculated as

$$L'_m = T'^2 \text{mass} \quad (18)$$

3.4 Chamber and Structural Member Model

The piezoelectric stack presses against the pumping chamber that is held in place by the structural body of the pump. Based on conservation of fluid, the pumping chamber can be described as

$$\frac{V_c}{\beta} \frac{dP_c}{dx} = A_c (\dot{x}_c + \dot{x}_s) + Q_{in} - Q_{out} - Q_{leakage} \quad (19)$$

where V_c is the volume of the fluid chamber, P_c is the chamber pressure and is equal to force applied to the chamber, F_c , divided by the area, A_c , of the chamber, β is the fluid bulk modulus, x_c and x_s are the displacements of the respective ends of the chamber, Q_{in} is the fluid coming into the chamber, Q_{out} is the fluid leaving the chamber, and $Q_{leakage}$ is the any stray leakage flows. Based on Newtonian mechanics, the chamber acceleration is proportional to the applied forces on the chamber, or

$$(M_c + M_p) \ddot{x}_c = F_p - F_c \quad (20)$$

where the effective mass of the piezoelectric stack, M_p , is 1/3 the total mass of the stack and M_c is the mass of chamber piston. Due to the low frequency of operation (below a few kilohertz), a lumped parameter model [8] for the pumping chamber is adequate because the acoustical wavelength is much larger than the overall piezoelectric stack. Likewise, the structural compliance forces can be represented as

$$M_s \ddot{x}_s + D_s \dot{x}_s + K_s x_s = -F_c \quad (21)$$

and where D_s is a structural damping term, K_s is the structural compliance, and M_s is the effective mass of the structure.

3.5 Actuator Model

The flow out of the pump will be fed to a hydraulic actuator. The actuator and load models are based on fluid conservation and Newtonian dynamics and are as follows:

$$Q_{out} = \frac{V_L}{\beta} \frac{dP_s}{dx} + A_L \dot{x}_m \quad (22)$$

and

$$M_L \ddot{x}_m = A_L P_s - B_v \dot{x}_m - M_L g \quad (23)$$

where V_L is the volume of the fluid in the actuator which varies as $V_L = V_{L0} + A_L x_m$ where x_m is the actuator position and V_{L0} is the initial fluid volume, M_L is the mass of the load, g is the gravitational constant, P_s is the actuator pressure, B_v is the fluid damping, and A_L is the effective area of the cylinder.

3.6 Valve Model

The last remaining model is for the valve and represents the most difficult aspect of the modeling problem. The fluid dynamic force on any valve results from a pressure drop across the valve. Its precise calculation would require a detailed fluid dynamic analysis of the entire flow pattern and an integration of the resultant pressure distribution over the valve. Due to the difficult nature of the problem presented, an approximate calculation of the force can be made by assuming that the pressure is uniformly equal to chamber pressure up to the minimum restriction and uniformly equal to the actuator or return pressure beyond this point. While such an abrupt change in static pressure is physically unrealizable, the resulting force calculation is useful in design (see [9] for a discussion of this model). Surprisingly, this fairly simple expression appears to adequately model the valve based on our test results; however, for detailed understanding of the problem, more elaborate methods based on computational fluid dynamics would have to be employed. The representation of the force on a single valve element, F_v , will be represented as

$$F_v = \left(1 - E_1 \frac{A_{12}}{A_s} \right) \Delta P A_s \quad (24)$$

where E_1 is a fixed constant (approximately close to 1 in value), A_s is the seat area which will equal $\pi d^2/4$ where d is the diameter of the hole, A_{12} is the flow area, ΔP is the pressures across the valve.

4.0 DESIGN OVERVIEW

Fig. 3 shows the overview drawing of the piezoelectric pump. The bottom piece contains an lvdt sensor used only for testing. Likewise, the top piece protruding out of the actuator is an optical sensor used to measure motion of the flappers. The same flapper design is used for the inlet and outlet ports; however, only half of the inlet flappers will be utilized. The balls that the flappers will hold in place (see Fig. 4) are made out of ruby sapphire with a density of 0.144 lbs/in³ which is one-half the density of steel. There are 15 holes for the high pressure flappers and 30 holes for the low pressure flappers.

Fig. 5 shows the two flapper locations in the pump. Material being used for the piston is an aluminum bronze material. Holes have been drilled inside the material to allow air to escape.

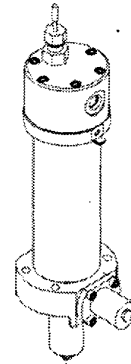


Figure 3. Overview drawing of the pump.

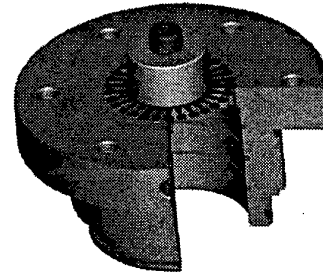


Figure 4. Piezoelectric pump valves (ruby balls under the flapper are not shown).

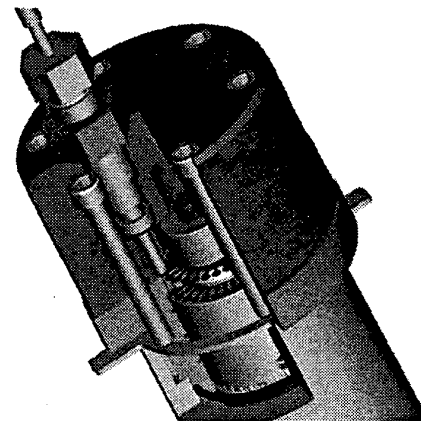


Figure 5. Cutaway showing the two flapper pieces (ruby balls under the flapper are not shown).

5. PERFORMANCE MEASUREMENTS OF PUMP COMPONENTS AND PUMP

5.1 Valve Performance

To verify the natural frequencies of the flapper design, actual flapper valves were fabricated and were clamped. An optical sensor was utilized to measure the ringing in the valve when the valves were displaced from equilibrium. The vibration tests of the flappers were captured by a data logging system and the results indicate that the valve can be designed at or above 2 kHz (see [4] for detail).

5.2 Pump Performance

ORNL has developed a novel hydraulic pump/actuator test bed (see Fig. 6), building upon the central idea of a distributive passive valving (see Fig. 7) scheme to achieve very high frequencies in moving small drops of fluid rapidly in and out of the pumping chamber.

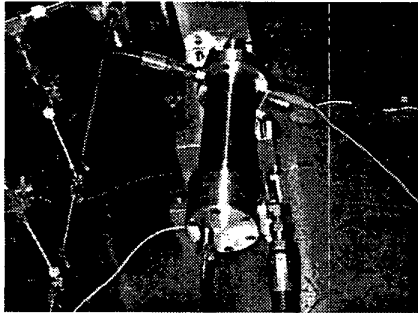


Figure 6. ORNL's piezoelectric pump.

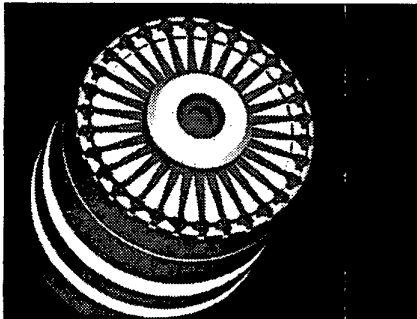


Figure 7. Distributive valves (head of flapper has been removed to show the ruby balls).

Due to our current power electronics limitation, the operational frequency that the stack could be driven could not exceed 400 Hz. For the final system, frequencies around 1 kHz are required and are currently being addressed. The following results, which benchmark the performance of ORNL's piezoelectric pump, will have to be linearly scaled to evaluate the overall performance potential of the pump. The first measurement is for no load flow test, where the test fluid is pumped into a fixed volume for 100 seconds. The theoretical and the measured flows are shown in Fig. 8 below.

Next, the deadhead pressure was tested by blocking the piston outlet flow. Theoretical pressures should exceed 1000 psi over a much larger frequency band than those shown in Fig. 9 (based on the assumed structural compliance and fluid bulk modulus values). There are two possible explanations for the discrepancies with the theoretical values: (1) leakage of the valves and (2) air that has not been properly evacuated or has become entrained into the working fluid.

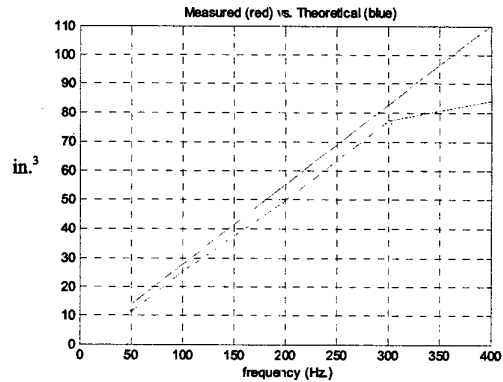


Figure 8. Flow (theoretical – top; actual – bottom).

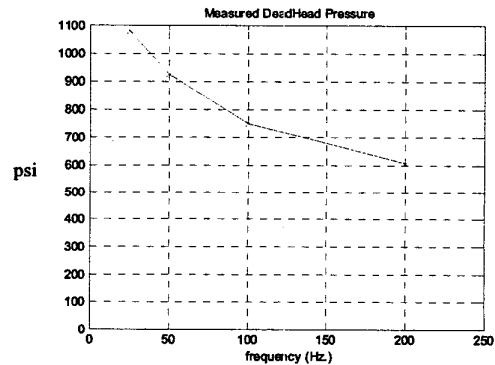


Figure 9. Deadhead pressure versus stack frequency.

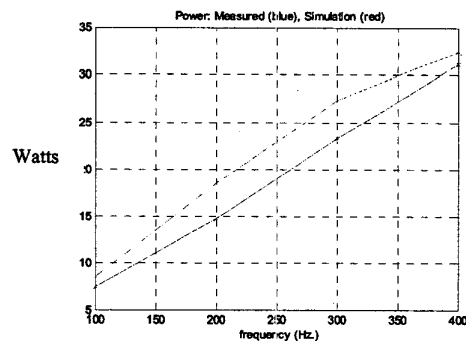


Figure 10. Power out of the piezoelectric pump for load of 650 psi and reservoir pressure of 50 psi (simulation is top curve, measured is bottom curve).

Figure 10 shows the results of a power test we have performed at various stack operating frequencies. This test entailed having the pump move fluid against a constant back pressure. Again due to the power electronic limitations, we are limited to tests around 300 to 400 Hz. As can be seen, we are roughly off by a factor of 3 from our design target (i.e., roughly 23 W at 300 Hz compared with the 67 W target goal).

Figs. 11 and 12 show the simulation and measured flapper displacement inside the pumping chamber.

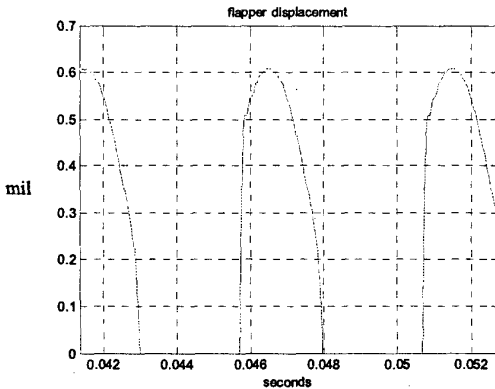


Figure 11. Simulation of flapper motion (200 Hz).

Variation of flapper displacement varied greatly: significantly more than shown in the Fig. 12 below. Note that the flapper is not closing as rapidly as in the simulation and appears to have a more square like peak than in the simulation.

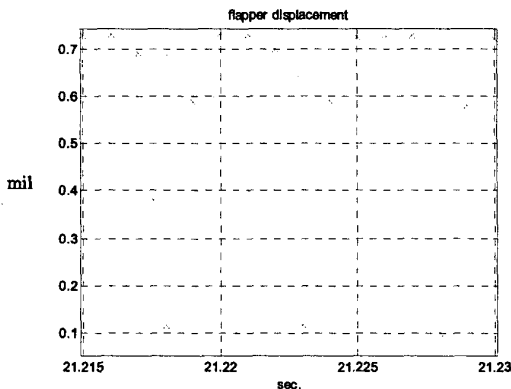


Figure 12. Measured flapper displacement (200 Hz).

Fig. 12 supports the conjecture that the valves are leaking fluid which diminishes the total potential power out of the pump.

6. CONCLUSIONS

A number of significant events have been achieved in the construction of a piezoelectric pump. Small drops of fluid can be controlled and directed by means of miniature valves. Understanding of the basic physics behind this novel pump has been developed that approximately match the general trends observed during the actual measurement of the pump. Very responsive valves have been designed and tested. While significant progress has been made on the construction of the piezoelectric pump, it appears that much more work is needed before it can compete with conventional electric motors in tandem with conventional hydraulic pumps. In particular, developing accurate models that would predict the overall passive valve behavior.

ACKNOWLEDGEMENT

The authors would like to thank Dr. John Main of the Defense Advanced Project Agency and Department of Energy's Office of Science under the KP Biological and Environmental Research Program.

REFERENCES

- [1] J. M. Hollerbach, I. W. Hunter, J. Ballantyne, "A Comparative Analysis of Actuator Technologies for Robotics," pp. 299-342 in *The Robotics Review 2*, ed. O. Khatib, J. Craig, T. Perez, The MIT Press, Cambridge, Massachusetts, 1992.
- [2] J. Jansen, et al., *Exoskeleton for Soldier Enhancement Systems Feasibility Study*, ORNL/TM-2000/256, Oak Ridge National Laboratory, Oak Ridge, Tenn., Sept. 2000.
- [3] K. Nasser, D., J. Leo, and H. H. Cudney, "Compact Piezohydraulic Actuation System," SPIE Paper Number 3991-41, 2000.
- [4] J. Jansen, et al., *Design, Analysis, Fabrication, and Testing of a Novel Piezoelectric Pump*, ORNL/TM-2003/188, Oak Ridge National Laboratory, Oak Ridge, Tenn., Oct. 2003.
- [5] Standards Committee of the IEEE Ultrasonics, Ferroelectrics, and Frequency Control Society, 1987, Std. 176-1987.
- [6] M. Goldfarb and N. Celanovic, "A Lumped Parameter Electromechanical Model for Describing the Nonlinear Behavior of Piezoelectric Actuators," *Journal of Dynamic Systems, Measurement, and Control*, Vol. 119, pp. 478-485 (1997).
- [7] H. E. Merritt, *Hydraulic Control Systems*, John Wiley and Sons, New York, 1967.
- [8] W. P. Mason, *Electromechanical Transducers and Wave Filters*, D. Van Nostrand Co., New York, 2nd edition, 1948.
- [9] B. W. Anderson, *The Analysis and Design of Pneumatic Systems*, Krieger Publishing Co., Malabar, Florida, 1967.